Active materials by four-dimension printing

Cite as: Appl. Phys. Lett. **103**, 131901 (2013); https://doi.org/10.1063/1.4819837
Submitted: 24 June 2013 . Accepted: 12 August 2013 . Published Online: 23 September 2013

Qi Ge, H. Jerry Qi, and Martin L. Dunn

Active materials by four-dimension printing

Qi Ge,[1] H. Jerry Qi,[1,a)] and Martin L. Dunn[2,b)]
[1]*Department of Mechanical Engineering, University of Colorado at Boulder, Boulder, Colorado 80309-0427, USA*
[2]*SUTD-MIT International Design Centre, Singapore University of Technology and Design, Singapore*

(Received 24 June 2013; accepted 12 August 2013; published online 23 September 2013)

We advance a paradigm of *printed active composite materials* realized by directly printing glassy shape memory polymer fibers in an elastomeric matrix. We imbue the active composites with intelligence via a programmed lamina and laminate architecture and a subsequent thermomechanical training process. The initial configuration is created by three-dimension (3D) printing, and then the programmed action of the shape memory fibers creates time dependence of the configuration—the four-dimension (4D) aspect. We design and print laminates in thin plate form that can be thermomechanically programmed to assume complex three-dimensional configurations including bent, coiled, and twisted strips, folded shapes, and complex contoured shapes with nonuniform, spatially varying curvature. The original flat plate shape can be recovered by heating the material again. We also show how the printed active composites can be directly integrated with other printed functionalities to create devices; here we demonstrate this by creating a structure that can assemble itself. © *2013 AIP Publishing LLC*. [http://dx.doi.org/10.1063/1.4819837]

Recent advances in additive manufacturing allow the precise placement of multiple materials at micrometer resolution with essentially no restrictions on the geometric complexity of the spatial arrangement. Complex three-dimension (3D) solids thus can be created with highly non-regular material distributions in an optimal fashion, enabling the fabrication of devices with unprecedented multifunctional performance. In this letter, we exploit these advances, to and introduce a paradigm of *printed active composites* (PACs, or active composites by four-dimension (4D) printing in the spirit of the recent developments of Tibbits,[1,2] although our work differs significantly in terms of the physical phenomena at play and the emphasis on understanding them). We directly print a composite from a CAD file that specifies the fiber architecture at the lamina and laminate level. This process has considerable design freedom to enable creation of composites with complex and controllable anisotropic thermomechanical behavior *via* the prescribed fiber architecture, shape, size, orientation, and even spatial variation of these parameters. Our PACs are *soft* composites consisting of glassy polymer fibers reinforcing an elastomeric matrix. The glassy polymer fibers exhibit the shape memory effect[3–7] and we use this to create *active* soft composites where the glassy polymer fibers serve as a switch to affect shape memory behavior of the composite.[8–11] In this manner, we imbue the active composites with intelligence *via* the lamina and laminate architecture and the thermomechanical training process. The extreme case of our approach is continuous, spatially varying material properties in a 3D domain, but here we limit ourselves to fiber/matrix lamina and laminates; indeed, this alone provides remarkable design freedom.

We start by creating printed lamina with prescribed fiber volume fractions and orientations, and characterize their anisotropic shape memory behavior. Guided by a nonlinear continuum theory that describes the behavior reasonably well, we then design the stacking sequence of lamina in laminates that can be thermomechanically programmed to assume complex three-dimensional configurations including bent, coiled, and twisted strips, folded shapes, and complex contoured shapes with nonuniform, spatially varying curvature. The original flat plate shape can be recovered by reheating the material. Finally, we use the PACs as hinges in a printed architecture to enable a self-folding box.

We realize the PAC concept *via* the processing approach shown in Figure 1(a). Briefly, we design the complete 3D architecture of the fibers and matrix in a CAD file to yield specific active behavior based on understanding developed from theory and simulation and use a 3D multimaterial polymer printer (Objet Connex 260, Stratasys, Edina, MN, USA) to print the composite. We design the matrix to be an elastomer and the fibers to be a glassy polymer with tailored thermomechanical, including shape-memory, behavior. The printing process works by depositing droplets of polymer ink at ~70 °C, wiping them into a smooth film, and then UV photopolymerizing the film.[12] This process results in a film that contains matrix and fiber material at an in-plane resolution of 32–64 μm, depending on the printing resolution. The complete composite architecture is then realized by printing multiple film layers to create an individual lamina and ultimately multiple layers to create the 3D laminate.

We design PACs that exhibit the shape memory effect over the range from $T_L = 15\,^{\circ}\mathrm{C}$ to $T_H = 60\,^{\circ}\mathrm{C}$. We use an elastomeric matrix in our work that has a glass transition temperature $T_g \sim -5\,^{\circ}\mathrm{C}$ and behaves as a rubbery solid between 10 and 100 °C with a modulus of ~0.7 MPa at 15 °C (it varies linearly with the change of temperature, and $E_s = 3nkT$ with $n = 5.1 \times 10^{25}\,\mathrm{m}^{-3}$ and k is Boltzmann constant). The fibers have a modulus of 3.3 MPa (13.3 MPa) at T_H (T_L) and $T_g \sim 35\,^{\circ}\mathrm{C}$ (supplementary material, Figure S1).[27] As a result, during a temperature cycle between T_L and T_H, the matrix is always rubbery, while the fibers undergo a glass transition

a)Electronic mail: qih@colorado.edu.
b)Electronic mail: martin_dunn@sutd.edu.sg.

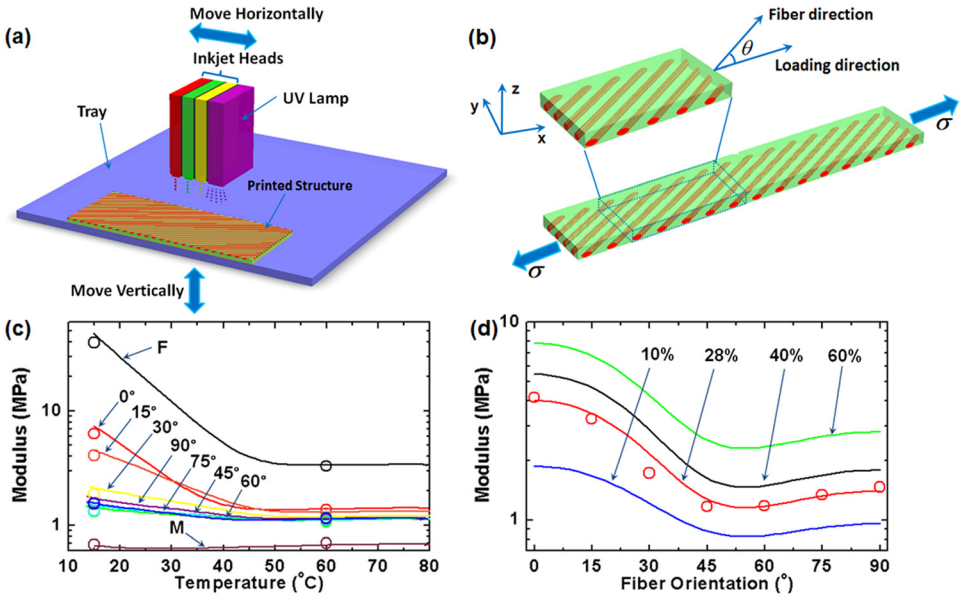

FIG. 1. (a) Schematic illustrating the PAC printing process. The inkjet heads move horizontally above the tray depositing multimaterial droplets of polymer ink at prescribed positions, wiping them into a smooth film, and then UV photopolymerizing the film. After one film layer is completed, the tray moves down to print the next layer. (b) Schematic of a PAC lamina; fibers are oriented at an angle θ from x-direction (the loading direction). (c) The storage modulus E_s in x-direction of the matrix (M), fiber (F), and the composites from 60 °C to 15 °C, along with the modulus obtained from quasi-static uniaxial tensile tests at 60 °C and 15 °C (circles). (d) Theoretical estimates of the relaxed modulus E_r versus fiber orientation, including experiments at $v_f = 0.28$ (circles) at 15 °C.

that enables their use as the switchable segment in the composite. We printed composite lamina (2 mm thick) with a single row of fibers (volume fraction $v_f = 0.28$) oriented at an angle θ (= 0°, 15°, 30°, 45°, 60°, 75°, and 90°) from the loading (x-) direction (Figure 1(b)).

We measured the storage modulus E_s of the matrix, fiber, and the composites in x-direction with a dynamic mechanical analyzer (DMA) as a function of temperature (Figure 1(c)). The matrix modulus decreases linearly with temperature, consistent with rubber entropic elasticity; the slight increase at 15 °C is because this is close to the glass transition region and continued decreases in temperature result in large increases in E_s (supplementary material, Figure S1).[27] The composites show an increasing modulus as temperature decreases, with a large variation centered at about 40 °C, which is associated with the glass transition of the fibers. Considerable anisotropy exists, especially as the fibers transition to the glassy state and stiffen. Also shown as circles in Figure 1(c) are results for the modulus obtained from quasi-static uniaxial tensile tests at 60 °C and 15 °C; they are in good agreement with the DMA results. Complete stress-strain curves are presented in supplementary material (Figure S2a and b)[27] and show linear response up to 1% strain. In uniaxial loading at 15 °C, the fibers exhibit significant stress relaxation, as do the composites with fiber-dominated behavior ($\theta = 0°$, 15°); the matrix does not exhibit stress relaxation and the composites with $\theta > 30°$ exhibit little stress relaxation (supplementary material, Figure S2c).[27] At 60 °C, none of the materials exhibit stress relaxation. The relaxation contributes importantly to the shape memory behavior of the composites.[13] In fact, the relaxed modulus E_r is more relevant to the resultant fixity of a shape memory material so in Figure 1(d) we plot the relaxed modulus (after 30 min) for each as a function of fiber orientation. Also shown are theoretical estimates (solid lines) based on a recent theory of fiber-reinforced elastomers (Guo *et al.*,[14,15] Lopez-Pamies *et al.*,[16] deBotton *et al.*;[17] supplementary material).[27] The theory describes the experiments well and both show significant anisotropy in the response; in many traditional composite applications this is not desired, but in active composites, we can exploit this anisotropy as additional design freedom.

To exercise the shape memory effect (Figure 2(a)), we deform samples at $T_H = 60$ °C which is above T_g of the fibers (~35 °C) and then maintain the applied stress on the sample while cooling it to $T_L = 15$ °C at a rate of 2 °C/min. At T_L, the matrix is still in the rubbery state but the fibers have transformed to the glassy state. During cooling, the strain decreases slightly, due to thermal strain of the constituents. After holding the sample at T_L for a time sufficient to equilibrate the strain (~5 min), we released the stress and observed elastic unloading, the magnitude of which depends on the fiber orientation. At this stage the composite is in its fixed configuration and we characterized the degree of fixity by $R_f = (\varepsilon_u - \varepsilon_T)/(\varepsilon_m - \varepsilon_T)$, where ε_m and ε_u are the axial strains before and after the unloading step, and ε_T is the thermal strain at T_L (supplementary material, Figure S2d).[27] Finally, we recover the strain by heating the unconstrained sample at 2 °C/min to 60 °C. Figure 2(b) shows the applied temperature and stress cycle and Figure 2(c) shows the strain response for the composites as well as for the fiber and matrix.

Figure 2(c) shows that there is significant anisotropy in the shape memory behavior of the composites as a function of fiber orientation; this is illustrated specifically for the fixity in Figure 2(d). The fixity as a function of θ follows the behavior of the relaxed modulus E_r, exhibiting a slight minimum at $\theta \sim 45$–60°. Predictions of a theoretical model, based on combining models of hyperelastic composites with those describing the shape memory behavior of glassy polymers are in good agreement with measurements for the shape memory cycle (supplementary material, Figure S3a–g)[27] and fixity (Figure 2(d)). We note that the polymer fibers themselves exhibit shape memory ($R_f \sim 80\%$), while the matrix does not ($R_f = 0\%$). Simulations show that fixity increases with increasing fiber volume fraction as this provides increasing stiffness to hold the composite in its prescribed deformation state after cooling. For all volume fractions, the fibers are most effective in terms of providing fixity when aligned with the load, but this is at the expense of reduced strain for a fixed stress.

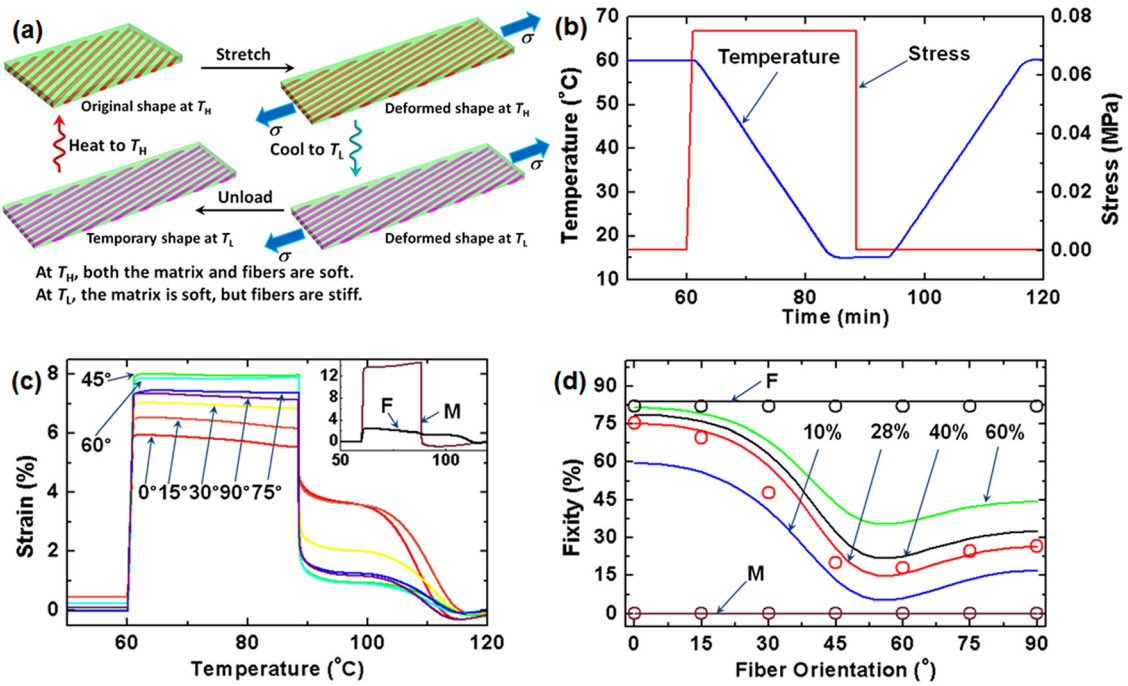

FIG. 2. Shape memory behavior of active composite lamina. (a) Schematic of a shape memory cycle. (b) Thermomechanical loading program for the shape memory behavior of the active composite lamina. (c) Strain-time response of the $v_f = 0.28$ composites (the inset denotes the matrix (M) and fibers (F)). (d) Predictions of fixity versus fiber orientation are compared to experiments (circles).

We exploit the anisotropic shape memory behavior of the active lamina to create PAC laminates in Figure 3. We design laminates with varying fiber orientations and volume fractions, and even allow these design parameters to vary within a lamina, an aspect that can be readily achieved via printing. Figure 3(a) shows the notional concept: a two-layer laminate with a prescribed fiber architecture is printed, then heated, stretched, cooled, and released. Upon release of the stress, it assumes a complex temporary shape, depending on the fiber architecture. Upon reheating it recovers its original shape, a flat rectangular strip. Figure 3(b) shows an actual strip in its original shape and then Figures 3(c)–3(h) show the results of this process with strips that are nominally identical macroscopically, but have differing fiber architectures. The laminates in Figures 3(c)–3(e) each have two layers of equal thickness (0.5 mm), one of them has a fiber volume fraction of $v_f = 0.25$ and the other is pure matrix ($v_f = 0$), and $\theta = 0°$, 90°, and 30° in Figures 3(c)–3(e), respectively. Both the $\theta = 0°$ and 90° strips roll into coils, with the $\theta = 0°$ having a much larger curvature due to the increased fixity of a $\theta = 0°$ lamina versus a $\theta = 90°$ lamina. In general, the magnitude of the curvature depends on the composite geometries and properties, the applied mechanical load, and the thermal history; all of these are design variables. The strip with $\theta = 30°$ coils into a helix due to the shear-tension coupling of the laminate; theoretical explanations for this basic behavior can be found in Chen *et al.*[18] as well as Huang *et al.*[19] The laminates of Figures 3(f)–3(h) have alternating regions of segments with two layers, one with fibers ($v_f = 0.25$) and the other without fibers ($v_f = 0$). The ordering of the segments is such that the fibers alternate from being in the top layer and bottom layer along the strip. In Figure 3(f), the fibers are at $\theta = 0°$ and so the strip assumes the shape of alternating bent segments, while in Figure 3(g), the fibers are at $\theta = 0°$ in the top layer and at $\theta = 30°$ in the bottom layer leading to a combination of bending and twisting of the strip in alternating fashion. In Figure 3(h), the fibers are all

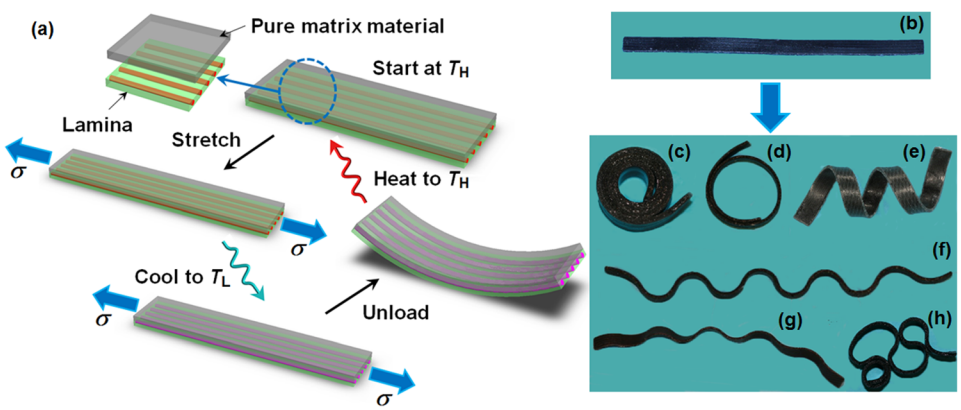

FIG. 3. Complex low-temperature shapes of active composite laminates obtained by design of the laminate architecture. (a) A two-layer laminate designed with one layer being a lamina with fibers at a prescribed orientation and one layer being pure matrix material is printed, then heated, stretched, cooled, and released. Upon release of the stress it assumes a complex shape, depending on the laminate architecture. When reheating it then assumes its original shape, a flat rectangular strip. (b) Shows an actual strip in its original shape and (c)–(h) show results of this process with differing fiber architectures.

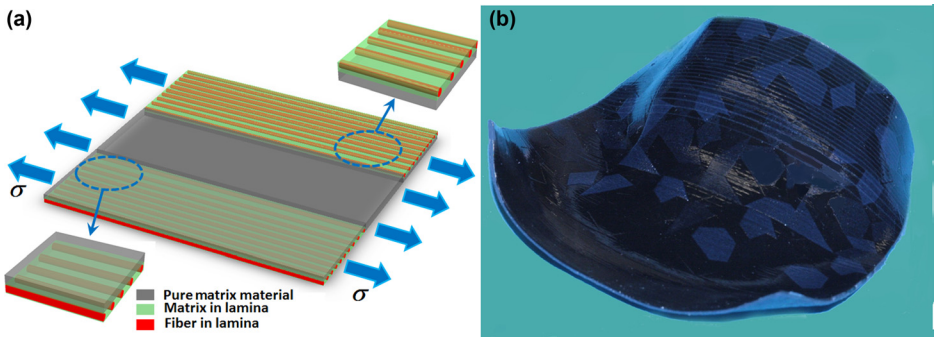

FIG. 4. A sculpted surface with a complex, nonuniform curvature obtained by design of the laminate architecture. (a) Schematic of a flat laminate that is stretched at T_H. (b) After cooling to T_L and unloading, a desired complex, nonuniform curvature is achieved.

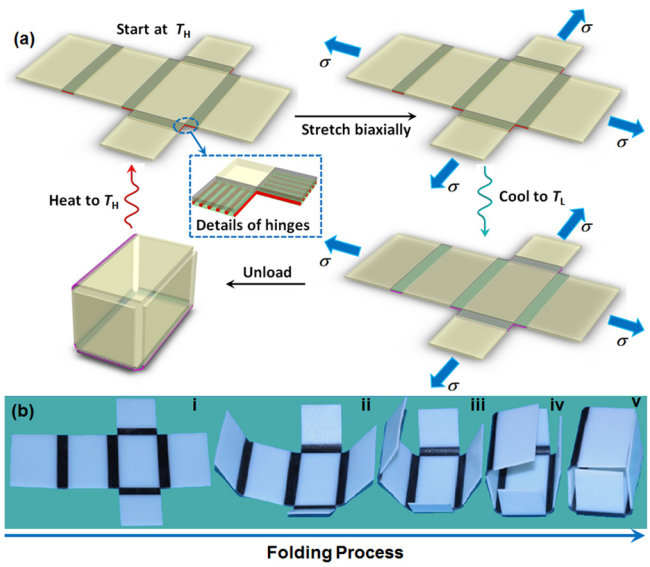

FIG. 5. A self-folding and opening box fabricated by the printing PACs as hinges connecting inactive plates of a stiff plastic. (a) Schematic of thermomechanical protocol to achieve the self-folding and opening box. (b) Photographs of the flat configuration folding to a closed box (i–vi).

at $\theta = 0^\circ$ but are patterned in segments along the strip of different lengths that lead to a variation of curvature in each segment.

Figure 4 shows an extension of this concept to realize a shape with complex, nonuniform curvature, essentially a sculpted surface. Here, a two-layer laminate (80 mm $\times$ 80 mm) is fabricated but the architecture of the fibers includes a spatial variation in both its orientation and volume fraction, to yield the desired curvature. Over each end of the laminate $\theta = 0^\circ$ fibers exist at a volume fraction that varies with position ranging from $v_f = 0.25$ at the end of the laminate to $v_f = 0.14$ toward the center of the laminate (the precise layout is shown in supplementary material).[27] The laminate is antisymmetric, with respect to the planar dimensions. The surface of the laminate has a randomly printed patchwork, intended to be reminiscent of the interesting artistic and architectural forms created by 3D printing by Oxman.[20] Unlike that complex surface that was directly printed in 3D, ours was created as a flat plate and then following our thermomechanical protocol, it assumed the curved shape as a result of the fibrous architecture. While the patchwork pattern here is only for aesthetic purposes, applications can be envisioned where the pattern has functional purposes.

Finally, in Figure 5, we show how the printed active composites can be integrated with other structural or functional components to create active devices. Here, two-layer PACs were printed to serve as hinges with six stiff plastic plates that are not intended to deform (the precise layout is shown in supplementary material).[27] After printing the flat configuration shown, we heat and stretch it biaxially. Upon cooling and release of the mechanical loads, it assembles into the closed box as shown in Figure 5.

In this paper, we demonstrated the concept of printed active composites and how they can be integrated with other printed components of arbitrary geometry and functionality. In our examples, we emphasized composites with glassy fibers in an elastomeric matrix, however, one can extend the concept to general spatial variations of materials properties and use computational design tools such as shape and topology optimization to design the layout of the materials in the composite,[21–24] as well as exploit instabilities to create large configurational changes.[25,26]

The authors gratefully acknowledge the support from an AFOSR grant, Program Manager, Dr. Byung-Lip "Les" Lee. H.J.Q. acknowledges the support from NSF CMMI-1334637. M.L.D. acknowledges support from the SUTD-MIT International Design Centre.

[1]S. Tibbits, Archit. Des. **82**, 68 (2012).
[2]S. Tibbits and K. Cheung, Assem. Autom. **32**, 216–225 (2012).
[3]Y. P. Liu, K. Gall, M. L. Dunn, A. R. Greenberg, and J. Diani, Int. J. Plast. **22**, 279 (2006).
[4]T. D. Nguyen, H. J. Qi, F. Castro, and K. N. Long, J. Mech. Phys. Solids. **56**, 2792 (2008).
[5]H. J. Qi, T. D. Nguyen, F. Castro, C. M. Yakacki, and R. Shandas, J. Mech. Phys. Solids. **56**, 1730 (2008).
[6]V. Srivastava, S. A. Chester, N. M. Ames, and L. Anand, Int. J. Plast. **26**, 1138 (2010).
[7]K. K. Westbrook, P. H. Kao, F. Castro, Y. F. Ding, and H. J. Qi, Mech. Mater. **43**, 853 (2011).
[8]Q. Ge, X. F. Luo, E. D. Rodriguez, X. Zhang, P. T. Mather, M. L. Dunn, and H. J. Qi, J. Mech. Phys. Solids. **60**, 67 (2012).
[9]X. F. Luo and P. T. Mather, Macromolecules **42**, 7251 (2009).
[10]E. D. Rodriguez, C. W. Weed, and P. T. Mather, Macromol. Chem. Phys. **214**, 1247 (2013).
[11]J. G. Boyd and D. C. Lagoudas, J. Intell. Mater. Syst. Struct. **5**, 333 (1994).
[12]L. J. Stiltner, A. M. Elliott, and C. B. Williams, in *Solid Freeform Fabrication Symp. Proc.*, 2011, Vol. 22, p. 583.
[13]K. Yu, T. Xie, J. S. Leng, Y. F. Ding, and H. J. Qi, Soft Matter **8**, 5687 (2012).
[14]Z. Y. Guo, X. Q. Peng, and B. Moran, J. Mech. Phys. Solids **54**, 1952 (2006).
[15]Z. Y. Guo, X. Q. Peng, and B. Moran, Int. J. Solids Struct. **44**, 1949 (2007).
[16]O. Lopez-Pamies and M. I. Idiart, J. Engrg. Math. **68**, 57 (2010).
[17]G. deBotton, I. Hariton, and E. A. Socolsky, J. Mech. Phys. Solids **54**, 533 (2006).
[18]Z. Chen, C. Majidi, D. J. Srolovitz, and M. Haataja, Appl. Phys. Lett. **98**, 011906 (2011).

[19]J. S. Huang, J. Liu, B. Kroll, K. Bertoldi, and D. R. Clarke, Soft Matter **8**, 6291 (2012).
[20]N. Oxman, Virtual Phys. Prototyp. **6**, 3 (2011).
[21]M. L. Dunn and K. Maute, Mech. Mater. **41**, 1083 (2009).
[22]M. Howard, J. Pajot, K. Maute, and M. L. Dunn, J. Microelectromech. Syst. **18**, 1137 (2009).
[23]J. M. Pajot, K. Maute, Y. H. Zhang, and M. L. Dunn, Int. J. Solids Struct. **43**, 1832 (2006).
[24]C. J. Rupp, A. Evgrafov, K. Maute, and M. L. Dunn, J. Intell. Mater. Syst. Struct. **20**, 1923 (2009).
[25]M. L. Dunn, Y. H. Zhang, and V. M. Bright, J. Membr. Sci. **11**, 372 (2002).
[26]Y. H. Zhang and M. L. Dunn, J. Mech. Phys. Solids **52**, 2101 (2004).
[27]See supplementary material at http://dx.doi.org/10.1063/1.4819837 for thermomechanical properties, theories of PAC lamina and detailed layouts of PAC laminates.